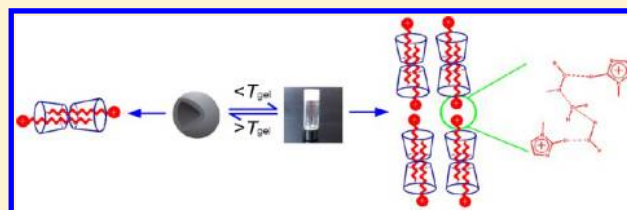


# Temperature-Induced Reversible Transition between Vesicle and Supramolecular Hydrogel in the Aqueous Ionic Liquid– $\beta$ -Cyclodextrin System

Jingjing Zhang and Xinghai Shen\*

Beijing National Laboratory for Molecular Sciences (BNLMS), Radiochemistry and Radiation Chemistry Key Laboratory of Fundamental Science, College of Chemistry and Molecular Engineering, Peking University, Beijing 100871, China

**ABSTRACT:** The vesicle is found to form in the concentrated aqueous solution of ionic liquid 1-dodecyl-3-methylimidazolium bromide ( $C_{12}mimBr$ ) and  $\beta$ -CD. By decreasing the temperature, the vesicle changes into a novel supramolecular hydrogel constructed from lamellae. The process is reversible and reproducible. The mechanism for the formation of vesicles and supramolecular hydrogel is studied by various methods. It is suggested that the main driving force is hydrogen bonding between  $\beta$ -CDs,  $\beta$ -CD and the solvent, the imidazolium headgroup of  $C_{12}mim^+$ , and the solvent. Accordingly, the basic structural features of the vesicle and supramolecular hydrogel based on ionic liquid and  $\beta$ -CD are illustrated. The structural evolution from vesicles to hydrogels is also discussed herein.



## INTRODUCTION

Ionic liquids (ILs), as a new class of molten salts at room temperature, have attracted increasing attention in recent years.<sup>1</sup> Because of their nonvolatile nature, they can prevent environmental pollution and can be used as environmentally benign solvents.<sup>2</sup> Furthermore, they have many other desirable properties, such as easy recyclability, nonflammability, high ionic conductivity, a wide electrochemical potential window, and high thermal stability, etc., making them important as novel solvents in organic synthesis, chemical separations, solar cells, and so on.<sup>3–6</sup> In the field of supramolecular chemistry, the performance of ILs is likewise remarkable. They can either participate directly in the assembly of supramolecular organizations or influence the assembly of various supramolecular structures in a certain way. In addition, there exist three-dimensional supramolecular networks with polar and nonpolar regions in imidazolium ILs, which can be used as powerful supramolecular receptors. Therefore, the study of ILs on supramolecular chemistry is fruitful and intriguing. Firestone et al. and Inoue et al.<sup>7,8</sup> studied the phase behavior of 1-decyl-3-methylimidazolium bromide ( $C_{10}mimBr$ ) and its mixture with water. They reported the formation of a stable, homogeneous hydrogel on the addition of water. It originates from a hydrogen-bonding network comprising water, bromide ion, and the imidazolium cation. However, with the addition of a suitable amount of alcohol, 1-octyl-3-methylimidazolium chloride ( $C_8mimCl$ ) can form the anisotropic  $L_\alpha$  phase.<sup>9</sup> The driving force originates from the hydrophobic force among the hydrocarbon chains and the hydrogen-bonding network comprising the imidazolium ring,  $Cl^-$ , water, and alcohols.

Cyclodextrins (CDs) can include various molecules in their cavities due to hydrophobic interactions and/or hydrogen bondings to form inclusion complexes.<sup>10,11</sup> The CD inclusion

complex is another important assembly in supramolecular chemistry and can be basal for more ordered supramolecular assembly. Our group previously reported the interaction pattern between imidazolium-based ILs and  $\beta$ -CD in aqueous solutions.<sup>12,13</sup> They can form various inclusion complexes, 1:1 (guest:host), 1:2, or the coexistence of 1:1 and 1:2 complexes. Because multiple interactions, including hydrophobic interactions and hydrogen bondings, exist in the IL–CD–water system, we have been trying to prepare certain kinds of highly ordered supramolecular organizations in the IL–CD systems, and the reports on the subject are scarce so far.

Among supramolecular organizations, supramolecular hydrogels have been of interest in recent years.<sup>14</sup> They are mainly formed from low molecular weight gelators, which manipulate noncovalent interactions to self-assemble and immobilize the solvent into a three-dimensional entangled network in different ways.<sup>15–19</sup> Usually, they are sensitive to external stimuli such as heat, light, pH, and chemicals and have potential as biodegradable materials in drug delivery systems and chemical sensors.<sup>20–22</sup> Therefore, the design and preparation of novel hydrogels, especially stimuli-responsive hydrogels, are challenging in the fields of both materials science and medicine.<sup>23</sup> CD-based supramolecular hydrogels usually can be sensitive to external stimuli, and the ways to form the hydrogels are diverse. Osakada et al.<sup>24</sup> have reviewed the studies on the gel formed by rotaxane and pseudorotaxanes, which are principal ways for CD hydrogels.<sup>25–28</sup> Besides, CD hydrogels can also be prepared by host–guest complexes (including complexes with or without polymer chains),<sup>20,29–31</sup> metal–ligand bonding,<sup>32</sup> and micro-

**Received:** September 6, 2012

**Revised:** January 12, 2013

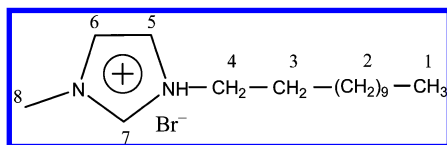
**Published:** January 12, 2013

tubes,<sup>33</sup> etc. Park et al.<sup>32</sup> have reported a novel  $\gamma$ -CD supramolecular hydrogel induced by lithium salt. The presence of threaded dye molecules inside the CD stacks facilitates the stabilization of the channel structure of CD. The hydrogen attraction between the lithium ions and the neighboring host  $\gamma$ -CD molecules helps the formation of the hydrogel. Nevertheless, there is no report on the CD-based supramolecular lamellar hydrogel, which is transformed from vesicles.

Vesicles are another important family of assembled structures. They are membrane-enclosed sacs at the nano- to microscales, which have found wide applications in biomedicine, nanomaterials, and drug and gene delivery.<sup>34,35</sup> Chemists have developed an ocean of amphiphilic molecular and macromolecular structures that spontaneously form vesicular structures,<sup>36</sup> among which CD-based supramolecular vesicles are significant because they are especially potential for the applications as drug carriers, nanoreactors, and so on.<sup>37</sup> There are mainly two methods to prepare the CD-based supramolecular vesicles: one is obtaining the amphiphilic CD surfactant by the modification of CD,<sup>38–40</sup> and the other is the self-assembly by the CD inclusion complex.<sup>41–44</sup> Comparing the two methods, the latter one has tremendous application potential. Jiang et al.<sup>45</sup> reported that sodium dodecyl sulfate (SDS) and  $\beta$ -CD can spontaneously form vesicles. For imidazolium-ILs with long alkyl side chains and  $\beta$ -CD, it can be supposed that they may also form vesicles.

Herein, we chose the IL 1-alkyl-3-methylimidazolium bromide ( $C_n$ mimBr, the structure of  $C_{12}$ mimBr is shown in Scheme 1) as the guest and studied the supramolecular

Scheme 1. Structure of  $C_{12}$ mimBr



assembly in the concentrated aqueous solutions of  $C_n$ mimBr- $\beta$ -CD. It was discovered that supramolecular hydrogels and vesicles can be prepared by the assembly of simple  $C_n$ mimBr- $\beta$ -CD inclusion complexes. According to the reports in the literature, different kinds of assemblies can be transformed by the change of various environmental factors,<sup>46–48</sup> and temperature often plays an important role in such transitions.<sup>49,50</sup> In the system, the vesicle phase can change into the lamellae hydrogel phase by the decrease of temperature. To our knowledge, this is the first report on CD-based supramolecular lamellar hydrogels containing ILs as well as transforming from the vesicle phase.

## EXPERIMENTAL SECTION

**Materials.**  $\beta$ -CD ( $\geq 98\%$  purity, Beijing Aoboxing) was recrystallized twice using tridistilled water and dried under vacuum for 24 h.  $C_6$ mimBr,  $C_8$ mimBr,  $C_{10}$ mimBr, and  $C_{12}$ mimBr ( $>99\%$  purity) were purchased from Lanzhou Institute of Chemical Physics (China). Analytical grade reagents urea and NaOH were used as received.  $D_2O$  (99.9% isotopic purity, Beijing Chemical Reagents Company) was used as a solvent in NMR measurements. Tridistilled water was used throughout the experiments.

**Instruments.** The UV analysis was recorded on a Hitachi 3010 UV-vis spectrometer. Dynamic light scattering (DLS)

measurements were performed on an ALV/DLS/SLS-S022F photo correlation spectrometer. For the freeze-fracture transmission electron microscopy (FF-TEM), the fracturing and replication were carried out in a freeze-fracture apparatus (Balzers BAF400, Germany) at  $-140$  °C. Pt/C was deposited at an angle of  $45^\circ$  to shadow the replicas, and C was deposited at an angle of  $90^\circ$  to consolidate the replicas. The resulting replicas were examined in a JEM-100CX electron microscope. TEM micrographs were obtained with a JEM-100CX II transmission electron microscope (working voltage of 80–100 kV). Differential scanning calorimeter (DSC) measurements were performed on a Q100 instrument upon heating or cooling the samples at the rate of  $1$  °C/min. The spectra of both  $^1H$  NMR and  $^1H$ - $^1H$  ROESY were recorded on Bruker AV400 MHz NMR spectrometer with a mixing time of 300 ms in the phase-sensitive mode for the latter. The morphologies of the samples were visualized by scanning electron microscopy (SEM) on 1910FE. Fourier transform infrared (FTIR) spectra were recorded on a NICOLET iN10 MX spectrometer at a frequency ranging from 600 to  $4000$   $cm^{-1}$ . Wide-angle X-ray diffraction (WAXRD) patterns were obtained at room temperature on a DMAX-2400 (Rigaku, Japan) diffractometer.

**Methods.** The  $C_{12}$ mimBr- $\beta$ -CD system was prepared by mixing an equal mole amount of  $C_{12}$ mimBr and  $\beta$ -CD, keeping the concentrations of both  $C_{12}$ mimBr and  $\beta$ -CD at  $0.25$  mol  $dm^{-3}$ . The sample was heated to a temperature of  $60$  °C and became a transparent and isotropic solution. A white hydrogel was obtained by cooling the solution below  $10$  °C, and the xerogel was obtained by quickly freezing the hydrogel with liquid nitrogen.

In the measurement of DLS, the wavelength of laser was 632.8 nm, and the scattering angle was  $90^\circ$ . The temperature was controlled at  $25$  °C. The samples were treated by centrifugation at 12000 rpm for 30 min before the measurement.

In the measurement of UV-vis, the temperature was controlled by placing the sample in a 1 cm path length cell compartment whose walls were accessible to water circulation. The samples were kept for at least 10 min to attain equilibrium, and the final temperature was obtained by a thermocouple (Check-temp, Hanna, Italy).

One drop of the sample solution was placed onto a Formvar-coated copper grid, and a uranyl acetate solution (2%) was used as the staining agent to make the TEM images more clear.

The Cu  $K\alpha$  radiation source ( $\lambda = 0.154041$  nm) was applied in the measurement of WAXRD. The supplied voltage and current were set to 40 kV and 100 mA, respectively. Powder samples were mounted on a sample holder and scanned from  $3$  to  $40^\circ$  of  $2\theta$  at a speed of  $5^\circ$ /min.

## RESULTS AND DISCUSSION

**Structures of the Supramolecular Assemblies.** *Characterization of the Vesicle.* Because  $C_{12}$ mimBr can form micelles in aqueous solution,<sup>51,52</sup> one may wonder whether other assemblies exist in the concentrated  $C_{12}$ mimBr- $\beta$ -CD system. Thus, we use DLS to study the assemblies in the solution. As shown in Figure 1, peaks with a mean hydrodynamic radius ( $R_h$ ) around 1.4 (correlative intensity, 93.3%) and 127 nm (correlative intensity, 6.7%) appear. González-Gaitano et al.<sup>53</sup> reported that the radius of monomeric  $\beta$ -CD is about 0.8 nm in the DLS experiment. Herein, the radius of 1.4 nm, which is slightly larger than that of monomeric  $\beta$ -CD, can be attributed to the formation of  $\beta$ -CD

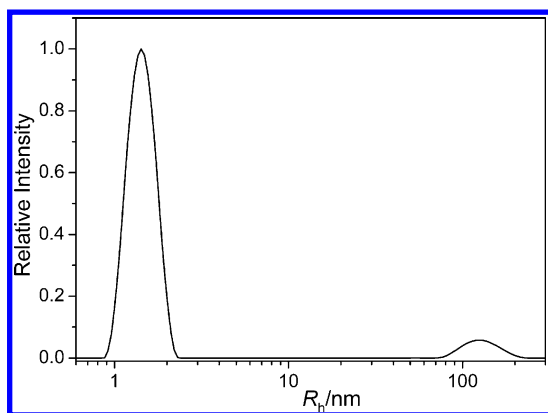


**Figure 1.** DLS result of the aqueous solution of  $C_{12}mimBr$  ( $0.25 \text{ mol dm}^{-3}$ )– $\beta$ -CD ( $0.25 \text{ mol dm}^{-3}$ ).

inclusion complexes. Besides, according to our previous report,<sup>13</sup> we can deduce that 1:1 (guest:host) and 1:2 inclusion complexes coexist between 1-dodecyl-3-methylimidazolium bromide and  $\beta$ -CD. The radius of 1.4 nm is maybe attributed to  $\beta$ -CD inclusion complexes. The radius of 127 nm is maybe attributed to either the incompact  $\beta$ -CD aggregates<sup>53</sup> or a certain kind of supramolecular assembly, for example, vesicles. González-Gaitano et al.<sup>53</sup> reported that  $\beta$ -CD is persistent in its aggregation even after sieving its solutions through  $0.02 \mu\text{m}$  filters, which displays a fast kinetics of the aggregates. However, when the mixture of  $C_{12}mimBr$  and  $\beta$ -CD is treated with  $0.2 \mu\text{m}$  filters, the peak of 127 nm disappears. It can be concluded that the radius of 127 nm is not attributed to incompact  $\beta$ -CD aggregates. Probably, there are some novel assemblies in the solution. From the TEM result in Figure 2a, we can observe the packed particles with diameters of about 50–80 nm as well as the separated particles (as shown in the inset) whose diameters are about 100 nm. In Jiang's work, they reported two coexisting populations of hollow vesicles with diameters of  $\sim 700$  and  $\sim 100$  nm in the system of  $SDS@2\beta$ -CD.<sup>45</sup> It should be reasonable that the vesicle structure in our system can be compatible with a high size polydispersity. As is shown in Figure 2a, the brightness of the brim and that of the center are different, indicating that the particles are hollow vesicles rather than mere solid particles. Besides, the phenomenon that some of the particles have burst (arrows in Figure 2a) also confirms the formation of vesicles. It is further certified by the FF-TEM result in Figure 2b, where both the dual-continuous phase of the vesicle and the separated vesicles can be observed.

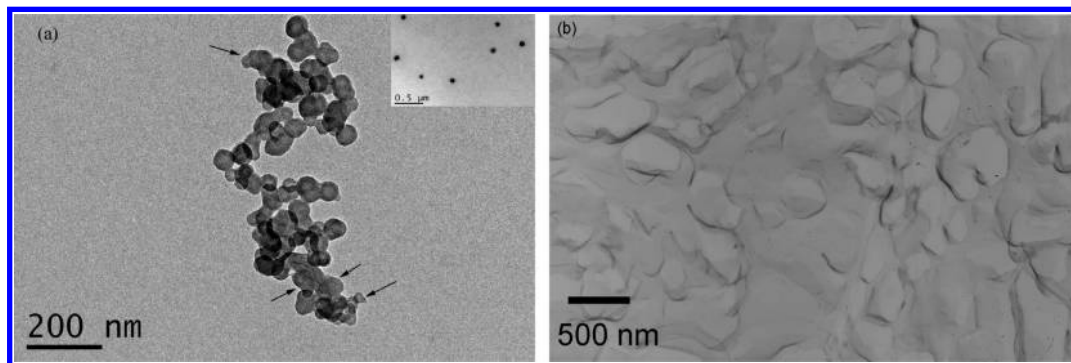


**Figure 2.** (a) TEM and (b) FF-TEM micrographs of the aqueous solution of  $C_{12}mimBr$  ( $0.25 \text{ mol dm}^{-3}$ )– $\beta$ -CD ( $0.25 \text{ mol dm}^{-3}$ ). The separated particles are shown in the inset of panel a. Arrows in panel a indicate the “broken” side of the vesicle.

Considering that DLS gives the statistical result of the size distributions, while TEM reflects the local result of the assemblies, one can see that the results obtained from the two methods generally coincide with each other. As most of the vesicles are packed together, it is reasonable that the peak of larger than 100 nm is very weak and even disappears when the solution is treated by centrifugation or by the filtration of a  $0.2 \mu\text{m}$  membrane.

**Characterization of the Supramolecular Hydrogel.** To understand the structure of the hydrogel, we also apply the method of FF-TEM to study the system. As is shown in Figure 3a, the hydrogel is the lamellae phase. Meanwhile, the xerogel is obtained and studied mainly by SEM, FTIR, and WAXRD. It can be seen from Figure 3b that the xerogel reveals the lamellae morphology, which coincides with the result of Figure 3a.

The FTIR spectra of  $\beta$ -CD,  $C_{12}mimBr$ , and  $C_{12}mimBr$ – $\beta$ -CD xerogel are shown in Figure 4. The spectrum of the xerogel is similar to that of  $\beta$ -CD, suggesting that the framework of the xerogel is  $\beta$ -CD, while only the weak signal  $2854 \text{ cm}^{-1}$  of the xerogel may indicate the presence of IL, suggesting that IL is included in the  $\beta$ -CD cavity. The spectrum of pure  $\beta$ -CD shows a broad band at  $3375 \text{ cm}^{-1}$ , which is assigned to symmetric and antisymmetric O–H stretching modes.<sup>54</sup> It shifts to a lower frequency at  $3356 \text{ cm}^{-1}$  because of the formation of the xerogel. It is well-known that the association of OH groups makes the stretching peak shift to a lower frequency.<sup>55</sup> The evident change of frequency herein clearly reflects the association of OH groups. We have measured the amount of residual solvent of the xerogel and found that the quantity of water is about 7% (w/w). It can be seen that the intermolecular interactions between  $\beta$ -CDs,  $\beta$ -CD and water may also contribute to the formation of the hydrogel.

The WAXRD patterns of  $\beta$ -CD,  $C_{12}mimBr$ , and the xerogel are shown in Figure 5. The major peaks at  $2\theta = 9.5, 12.8, 13.4,$  and  $18.2^\circ$  are observed in the  $\beta$ -CD pattern, indicating the existence of a typical cage structure.<sup>56</sup> The xerogel has a different pattern relative to  $\beta$ -CD and  $C_{12}mimBr$ . In this pattern, the major peaks appear at  $2\theta$  values of  $5.52$  and  $11.08^\circ$ , corresponding to  $d$  spacings of  $15.99$  and  $7.98 \text{ \AA}$ , respectively. The value  $7.98 \text{ \AA}$  is close to the characteristic value of the height of  $\beta$ -CD, indicating that the basic structure of the host is well maintained.<sup>57</sup> The value  $15.99 \text{ \AA}$  is exactly twice as large as the  $d$  spacing of  $7.98 \text{ \AA}$ , which strongly suggests that  $\beta$ -CD molecules with the number of  $2n$  ( $n \geq 1$ ) to construct the basic model of the supramolecular gel.



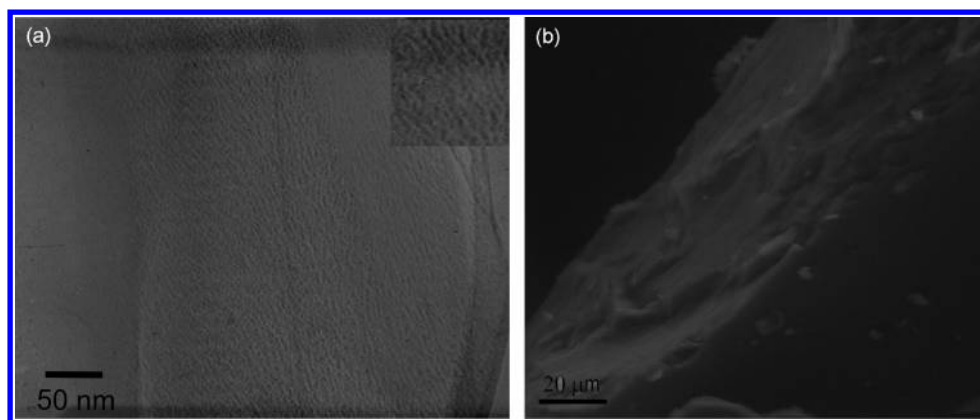


Figure 3. (a) FF-TEM image of  $C_{12}\text{mimBr}-\beta\text{-CD}$  hydrogel and (b) SEM image of xerogel.

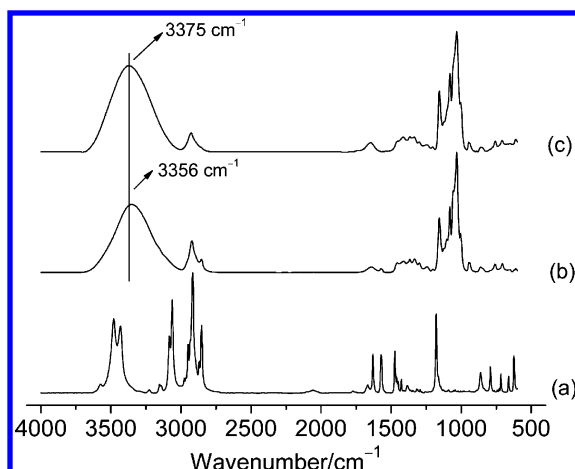


Figure 4. FTIR absorption spectra of (a)  $C_{12}\text{mimBr}$ , (b) xerogel, and (c)  $\beta\text{-CD}$ .

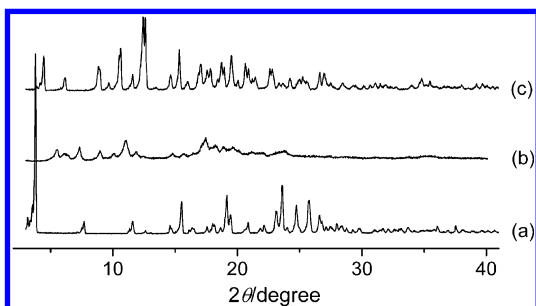


Figure 5. WAXRD patterns of (a)  $C_{12}\text{mimBr}$ , (b) xerogel, and (c)  $\beta\text{-CD}$ .

**Characterization of the Transformation between Vesicle and Hydrogel.** As is shown in Figure 6, the sol-to-gel transition is monitored by the absorbance at 650 nm in UV-vis spectroscopy, as there is no absorbance at 650 nm for the aqueous solution of either  $C_{12}\text{mimBr}$  or  $\beta\text{-CD}$ . A dramatic increase in absorbance and viscosity is observed with the decrease of the temperature. Finally, the opaque solution becomes nonflowing at 13 °C, yielding the required white hydrogel as shown in Figure 6. The temperature 13 °C corresponds to that of the sol-gel transition ( $T_{\text{gel}}$ ). With the increase of the temperature, the absorbance at 650 nm decreases greatly, and the hydrogel begins to flow and finally becomes a transparent solution again above 15 °C (gel-to-sol). The two curves of both heating and cooling processes are

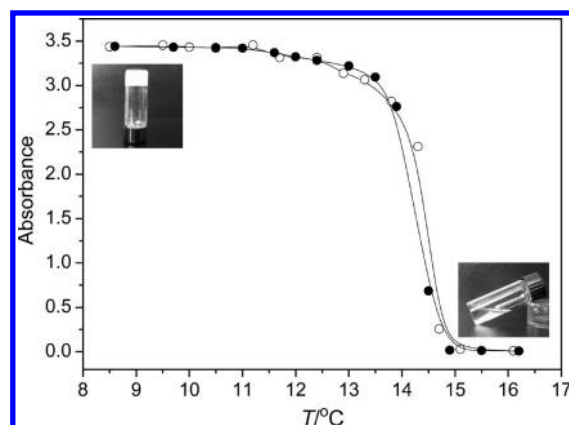


Figure 6. Sol-to-gel (●) and gel-to-sol (○) transition in the aqueous solution of  $C_{12}\text{mimBr}$  ( $0.25 \text{ mol dm}^{-3}$ )- $\beta\text{-CD}$  ( $0.25 \text{ mol dm}^{-3}$ ) monitored by the absorbance at 650 nm.

almost coincided, indicating that the sol-gel transition is reversible.

The phase transition from vesicle to lamellae hydrogel should accompany a heat effect. Therefore, DSC measurements are employed to monitor the temperature-dependent phase transition. As shown in Figure 7, for the sample of 5.13 mg in the DSC cell, an endothermic peak in the heating curve and an exothermic peak in the cooling curve can be observed. The endothermic peak of 14.7 °C and exothermic peak of 13.2 °C correspond to the dramatic decrease and increase of the

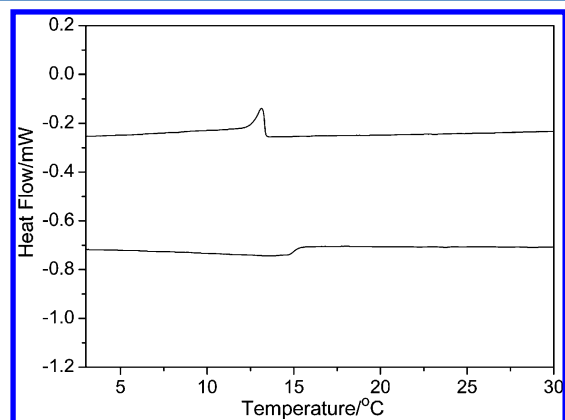


Figure 7. DSC heating and cooling curves of aqueous solutions of  $C_{12}\text{mimBr}$  ( $0.25 \text{ mol dm}^{-3}$ )- $\beta\text{-CD}$  ( $0.25 \text{ mol dm}^{-3}$ ).

absorbance in Figure 6, respectively. It is possibly a result of the negative transfer enthalpy ( $\Delta H$ ) of vesicle to hydrogel transition, which provides strong support for the phase transition by the change of temperature. The estimated value  $\Delta H$  is  $-1.0 \pm 0.2$  J/g. The  $T_{\text{gel}}$  13.2 °C is identical with that obtained by UV-vis spectroscopy. Several heating-cooling cycles have been performed on the same sample, and the results are reproducible, which indicates the reversibility of the transition. Such a transition temperature is also remarkably influenced by the molar ratio of  $C_{12}\text{mimBr}$  to  $\beta\text{-CD}$  and the total concentration of  $C_{12}\text{mimBr}$  and  $\beta\text{-CD}$ . We can see that in Table 1, when the molar ratio of  $C_{12}\text{mimBr}$  to  $\beta\text{-CD}$  is less than

**Table 1.**  $T_{\text{gel}}$  Influenced by the Molar Ratio of  $C_{12}\text{mimBr}$  to  $\beta\text{-CD}$  and the Total Concentration of  $C_{12}\text{mimBr}$  and  $\beta\text{-CD}$  When the Molar Ratio of  $C_{12}\text{mimBr}$  to  $\beta\text{-CD}$  Is 1:1 ( $T_{\text{gel}}$  Is Measured by DSC)

molar ratio of $C_{12}\text{mimBr}$ to $\beta\text{-CD}$	2:1	3:2	1:1	2:3 <sup>a</sup>	1:2 <sup>a</sup>
$T_{\text{gel}}$ (°C)	10.0	11.1	13.2		
total concentration of $C_{12}\text{mimBr}$ and $\beta\text{-CD}$ (mol dm <sup>-3</sup> )	0.4	0.5	0.6	0.8	1
$T_{\text{gel}}$ (°C)	7.6	13.2	20.8	31.4	41.2

<sup>a</sup>The gel cannot be formed.

1:1, that is, the amount of  $\beta\text{-CD}$  surpasses that of  $C_{12}\text{mimBr}$ , the hydrogel cannot be formed. On the other hand, when keeping the molar ratio of  $C_{12}\text{mimBr}$  to  $\beta\text{-CD}$  at 1:1, the transition temperature increases with the promotion of the total concentration. When the total concentration is 1 mol dm<sup>-3</sup>, the transition temperature can be higher than 40 °C. The phenomenon can be applied to prepare specific hydrogels with lower or higher transition temperatures.

**Mechanism of Formation of the Supramolecular Assemblies.** *Mechanism of Formation of the Vesicle and Hydrogel.* Effects of different alkyl side chain of  $C_n\text{mimBr}$  ( $n = 6, 8, \text{ or } 10$ ) and the anion on the hydrogel formation have been studied (Table 2). The formation of vesicle is verified by the

**Table 2.** Formation of Vesicle and Hydrogel in Different Systems of Guest and  $\beta\text{-CD}$ <sup>a</sup>

	vesicle	hydrogel	the total concentrations of guest and $\beta\text{-CD}$ (mol dm <sup>-3</sup> )
$C_6\text{mimBr}-\beta\text{-CD}$	NF <sup>b</sup>	NF	0.5
$C_8\text{mimBr}-\beta\text{-CD}$	F <sup>b</sup>	F	0.5
$C_{10}\text{mimBr}-\beta\text{-CD}$	F	F	0.5
$C_{12}\text{mimBr}-\beta\text{-CD}$	F	F	0.5
CTAB- $\beta\text{-CD}$	F	NF	0.5
$C_{12}\text{mimCl}-\beta\text{-CD}$	F	F	0.3
$C_{12}\text{mimBF}_4-\beta\text{-CD}$	NF	NF	0.2

<sup>a</sup>The concentrations for the samples are maximal values to get transparent and isotropic solutions when keeping the molar ratio of guest and  $\beta\text{-CD}$  1:1. <sup>b</sup>F, formation; NF, cannot form.

method of TEM. It is discovered that both of the concentrated  $C_8\text{mimBr}-\beta\text{-CD}$  and  $C_{10}\text{mimBr}-\beta\text{-CD}$  systems can form vesicles and hydrogels, while the mixture of  $C_6\text{mimBr}$  and  $\beta\text{-CD}$  is precipitated, indicating that the long side chain is necessary for the formation of the assemblies. By changing the anion of IL, it is discovered that the  $C_{12}\text{mimCl}-\beta\text{-CD}$  system can form vesicles and hydrogels, while the  $C_{12}\text{mimBF}_4-\beta\text{-CD}$

system cannot form either vesicles or hydrogels. It is suggested that the anion that can interact with  $\beta\text{-CD}$  may disturb the formation of the vesicles and hydrogels.

Figure 8 shows the <sup>1</sup>H NMR spectra of both  $C_{12}\text{mimBr}$  (0.25 mol dm<sup>-3</sup>) and that upon addition of equal mole of  $\beta\text{-CD}$  in

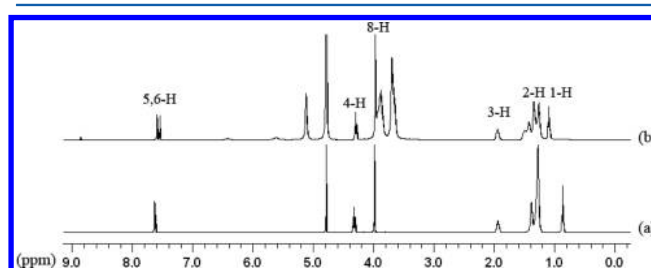


**Figure 8.** <sup>1</sup>H NMR signals of (a)  $C_{12}\text{mimBr}$  (0.25 mol dm<sup>-3</sup>) and (b)  $C_{12}\text{mimBr}$  (0.25 mol dm<sup>-3</sup>)- $\beta\text{-CD}$  (0.25 mol·dm<sup>-3</sup>) in  $D_2O$  at a temperature of 25 °C.

$D_2O$ . The signals at both  $\delta = 0.86$  ppm (Figure 8a) and 1.1 ppm (Figure 8b) are assigned to 1-H, while the signals at  $\delta = 1.2-1.6$  ppm to 2-H and  $\delta = 1.9$  ppm to 3-H (Scheme 1). The addition of  $\beta\text{-CD}$  leads to the obvious downfield shift of 1-H, 2-H, and 3-H, indicating the accommodation of the alkyl side chain of  $C_{12}\text{mimBr}$  by the cavity of  $\beta\text{-CD}$ . We have studied the interaction between IL and  $\beta\text{-CD}$  in aqueous solutions and found that only the alkyl side chain of the IL enters the cavity of  $\beta\text{-CD}$ .<sup>12,13</sup> It is coincident that when the vesicle is formed, the hydrophobic part of  $C_{12}\text{mimBr}$  is complexed by  $\beta\text{-CD}$  and the imidazolium ring stays outside the  $\beta\text{-CD}$  cavity. The 4-H, 5-H, 6-H, and 8-H of  $C_{12}\text{mimBr}$  shift upfield with the addition of  $\beta\text{-CD}$ , reflecting that the environment for the hydrogens gets more hydrophilic.

For the formation of supramolecular hydrogels, the driving forces can be van der Waals interactions, electrostatic interactions,<sup>16</sup>  $\pi-\pi$  interactions,<sup>20,58</sup> hydrophobic interactions,<sup>17</sup> and hydrogen bonding,<sup>19,30,58</sup> etc.,<sup>59,60</sup> among which the hydrogen bonding plays a major role.<sup>15</sup> Because <sup>1</sup>H-<sup>1</sup>H ROESY is generally employed to study the noncovalent interaction in supramolecular systems,<sup>61</sup> we study the interaction between  $C_{12}\text{mimBr}$  and  $\beta\text{-CD}$  in  $D_2O$  by the method (see Figure 9). The resonance correlations marked with a square suggest the formation of hydrogen bonding between the secondary hydroxyl group of  $\beta\text{-CD}$  and  $D_2O$ . Because of deprotonation of CD and loss of hydrogen bonding at a high pH, the effect of pH on the formation of vesicles and hydrogel has been studied by adding NaOH to the  $C_{12}\text{mimBr}-\beta\text{-CD}$  system. It is found that neither vesicles nor hydrogel was formed at pH > 13.

For comparison, the cationic surfactant, for example, hexadecyl trimethyl ammonium bromide (CTAB), whose structure is similar to that of  $C_{12}\text{mimBr}$  except the imidazolium headgroup, is tested. It is discovered that CTAB and  $\beta\text{-CD}$  can form the vesicle, whereas they cannot form the hydrogel (Table 2). This implicates that the imidazolium headgroup plays an important role in the hydrogel formation. Firestone et al.<sup>62</sup> reported the formation of a hydrogel by self-assembly of poly(1-(8-(acryloyloxy)octyl-3-methylimidazolium chloride) and suggested that it mainly arises from the hydrogen bonding between the imidazolium headgroup and the solvent. It is believed that the hydrogen bonding between the imidazolium headgroup of  $C_{12}\text{mim}^+$  and water contributes a lot to the formation of the hydrogel. Thus, we can deduce that the

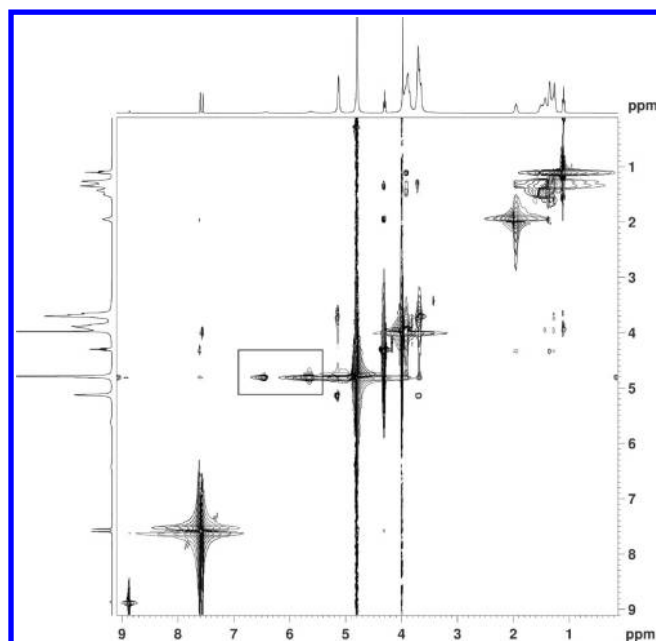


**Figure 9.**  $^1\text{H}$ – $^1\text{H}$  2D ROESY NMR spectrum of the  $\text{C}_{12}\text{mimBr}$  ( $0.25 \text{ mol dm}^{-3}$ )– $\beta\text{-CD}$  ( $0.25 \text{ mol dm}^{-3}$ ) in  $\text{D}_2\text{O}$  at 400 MHz and  $T_m = 300 \text{ ms}$  and  $T = 298 \text{ K}$ .

hydrogen-bonding interactions between the secondary hydroxyl group of  $\beta\text{-CD}$  and  $\text{H}_2\text{O}$ , and the imidazolium headgroup of  $\text{C}_{12}\text{mim}^+$  and  $\text{H}_2\text{O}$  drive the formation of the vesicles and hydrogels, which is usually the driving force for the self-assembly in semiconcentrated or concentrated surfactant systems.<sup>63</sup> Comparing the gels between IL–water and IL–CD–water herein, the former arises from diminution of hydrogen bonding between the imidazolium ring and the bromide counterion and the concomitant formation of a hydrogen-bonding network comprising water, bromide ion, and the imidazolium cation,<sup>7,8</sup> while the latter is constructed by the lamellae phase, which is higher ordered than the former one. The process of the formation of the  $\text{C}_{12}\text{mimBr}$ – $\beta\text{-CD}$  supramolecular hydrogel is similar to that of  $\gamma\text{-CD}$  hydrogel induced by lithium salt.<sup>32</sup>

**Structural Evolution from Vesicles to Hydrogels.** As is shown in Figure 7, during the transformation from vesicle to hydrogel, the heat effect is very small. It can be deduced that the models of vesicle and lamellar hydrogel are based on the same bilayer structure of  $\text{C}_{12}\text{mimBr}$ – $\beta\text{-CD}$ . From the result of WAXRD, we can deduce that  $\beta\text{-CD}$  molecules with the number of  $2n$  ( $n \geq 1$ ) exist in the basic model. Meanwhile, we observe the resonance correlations between 2-H and 4-H of  $\text{C}_{12}\text{mimBr}$ ,

indicating the intersection of two alkyl side chains of the IL molecules. Combining the height of  $\beta\text{-CD}$  cavity with the length of the alkyl chain of IL, it is deduced that two  $\beta\text{-CD}$ s construct the basic model. Accordingly, the structures of vesicle and the hydrogel are illustrated in Scheme 2. The sole  $\text{C}_{12}\text{mimBr}$  forms micelle, while the vesicles are formed on the addition of  $\beta\text{-CD}$ . The possible reasons for the formation of vesicles are that, according to the theory of critical-packing parameters,<sup>64</sup> the complexation of the alkyl side chain of  $\text{C}_{12}\text{mimBr}$  by  $\beta\text{-CD}$  results in the increase of the volume of the hydrocarbon tail. As a result, it is maybe inclined to form the structure of bilayer. On the other hand, the addition of  $\beta\text{-CD}$  modulates the balance of hydrophilicity and lipophilicity, which makes the vesicles stable at a relatively high temperature. With the decrease of temperature, the vesicle is changed into the lamellae, a higher ordered assembly as compared with vesicle. It has been reported that by increasing the temperature, a higher ordered state to a lower ordered one usually occurs among organized assemblies;<sup>50</sup> contrarily, a lower ordered assembly organizes to a higher ordered assembly by decreasing the temperature. Moreover, a negative enthalpy contributes to the transition from the vesicle to hydrogel. The report that the transition from vesicle to lamellar hydrogel or from lamellar hydrogel to vesicle is scarce and the present study may shed more light on the supramolecular hydrogels.

## CONCLUSIONS

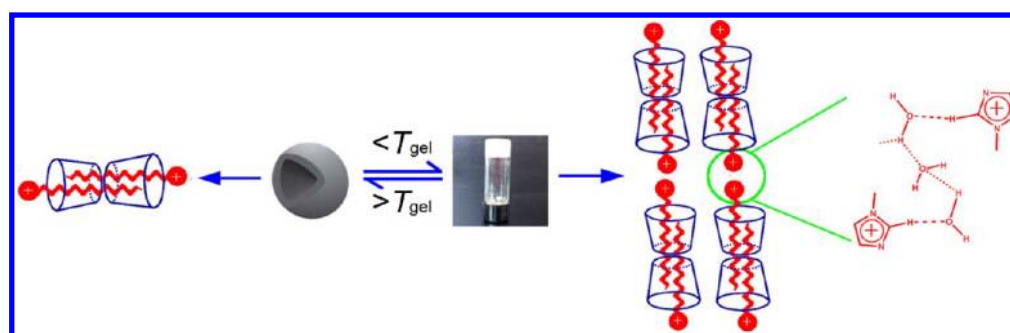
The concentrated mixtures of  $\text{C}_{12}\text{mimBr}$  and  $\beta\text{-CD}$  in aqueous solutions can form the vesicle, which can transform into the higher ordered assembly, a novel lamellae hydrogel, upon the decrease of temperature. The process is reversible, and the transition temperature can be obtained by UV–vis spectroscopy. It is discovered that with the concentration increase of  $\text{C}_{12}\text{mimBr}$ – $\beta\text{-CD}$ , the transition temperature also increases. We study the mechanism of the formation of the vesicle and hydrogel. The hydrogen-bonding interactions between  $\beta\text{-CD}$ s,  $\beta\text{-CD}$  and water, and the imidazolium headgroup of  $\text{C}_{12}\text{mim}^+$  and water contribute to the formation of vesicles and hydrogels. Combined with the study of the xerogel, one can obtain the model of vesicles and hydrogels. Such a hydrogel property may be useful in the field of biomedical applications, especially injectable drug delivery systems, as well as for understanding the gel structure and gelation mechanism.

## AUTHOR INFORMATION

### Corresponding Author

\*Tel: 86-10-62765915. Fax: 86-10-62759191. E-mail: xshen@pku.edu.cn.

**Scheme 2.** Schematic Diagram of the Vesicle and Lamellae Gel Formed by  $\text{C}_{12}\text{mimBr}$  and  $\beta\text{-CD}$





## Notes

The authors declare no competing financial interest.

## ACKNOWLEDGMENTS

We are grateful to Zheng Rong (Analytical Instrument Center of Peking University) for her help in DLS measurement and Jingxin Yang (Beijing NMR Center) for his help in NMR measurement. This work was financially supported by National Natural Science Foundation of China (Grant No. 20871009).

## REFERENCES

- (1) Hallett, J. P.; Welton, T. *Chem. Rev.* **2011**, *111*, 3508–3576.
- (2) Wilkes, J. S. *Green Chem.* **2002**, *4*, 73–80.
- (3) Welton, T. *Chem. Rev.* **1999**, *99*, 2071–2083.
- (4) Opallo, M.; Lesniewski, A. *J. Electroanal. Chem.* **2011**, *656*, 2–16.
- (5) Xu, C.; Yuan, L.; Shen, X.; Zhai, M. *Dalton Trans.* **2010**, *39*, 3897–3902.
- (6) Zhang, J.; Shen, X.; Chen, Q. *Curr. Org. Chem.* **2011**, *15*, 74–85.
- (7) Firestone, M. A.; Dzielawa, J. A.; Zapol, P.; Curtiss, L. A.; Seifert, S.; Dietz, M. L. *Langmuir* **2002**, *18*, 7258–7260.
- (8) Inoue, T.; Dong, B.; Zheng, L.-Q. *J. Colloid Interface Sci.* **2007**, *307*, 578–581.
- (9) Zhang, G. D.; Chen, X.; Zhao, Y. R.; Xie, Y. Z.; Qiu, H. Y. *J. Phys. Chem. B* **2007**, *111*, 11708–11713.
- (10) Szejtli, J. *Chem. Rev.* **1998**, *98*, 1743–1753.
- (11) Wenz, G. *Angew. Chem.-Int. Edit.* **1994**, *33*, 803–822.
- (12) He, Y. F.; Chen, Q. D.; Xu, C.; Zhang, J. J.; Shen, X. H. *J. Phys. Chem. B* **2009**, *113*, 231–238.
- (13) Zhang, J.; Shen, X. *J. Phys. Chem. B* **2011**, *115*, 11852–11861.
- (14) Sangeetha, N. M.; Maitra, U. *Chem. Soc. Rev.* **2005**, *34*, 821–836.
- (15) Estroff, L. A.; Hamilton, A. D. *Chem. Rev.* **2004**, *104*, 1201–1217.
- (16) Long, P. F.; Hao, J. C. *Soft Matter* **2010**, *6*, 4350–4356.
- (17) Menger, F. M.; Peresypkin, A. V. *J. Am. Chem. Soc.* **2003**, *125*, 5340–5345.
- (18) Ran, X.; Wang, H.; Zhang, P.; Bai, B.; Zhao, C.; Yu, Z.; Li, M. *Soft Matter* **2011**, *7*, 8561–8566.
- (19) You, L. Y.; Wang, G. T.; Jiang, X. K.; Li, Z. T. *Tetrahedron* **2009**, *65*, 9494–9504.
- (20) Ogoshi, T.; Takashima, Y.; Yamaguchi, H.; Harada, A. *J. Am. Chem. Soc.* **2007**, *129*, 4878–4879.
- (21) Bilensoy, E.; Moroy, P.; Cirpanh, Y.; Bilensoy, T.; Calis, S.; Mollamahmutoglu, L. *J. Inclusion Phenom. Macrocyclic Chem.* **2011**, *69*, 309–313.
- (22) Truong, W. T.; Su, Y.; Meijer, J. T.; Thordarson, P.; Braet, F. *Chem.-Asian J.* **2011**, *6*, 30–42.
- (23) Banerjee, S.; Das, R. K.; Maitra, U. *J. Mater. Chem.* **2009**, *19*, 6649–6687.
- (24) Suzuki, Y.; Taira, T.; Osakada, K. *J. Mater. Chem.* **2011**, *21*, 930–938.
- (25) Sabadini, E.; Cosgrove, T.; Taweeprada, W. *Langmuir* **2003**, *19*, 4812–4816.
- (26) Liu, K. L.; Zhu, J. L.; Li, J. *Soft Matter* **2010**, *6*, 2300–2311.
- (27) Tomatsu, I.; Hashidzume, A.; Harada, A. *Macromol. Rapid Commun.* **2005**, *26*, 825–829.
- (28) Nogueiras-Nieto, L.; Alvarez-Lorenzo, C.; Sandez-Macho, I.; Concheiro, A.; Otero-Espinar, F. J. *J. Phys. Chem. B* **2009**, *113*, 2773–2782.
- (29) Takashima, Y.; Nakayama, T.; Miyauchi, M.; Kawaguchi, Y.; Yamaguchi, H.; Harada, A. *Chem. Lett.* **2004**, *33*, 890–891.
- (30) Deng, W.; Yamaguchi, H.; Takashima, Y.; Harada, A. *Chem.-Asian J.* **2008**, *3*, 687–695.
- (31) Deng, W.; Yamaguchi, H.; Takashima, Y.; Harada, A. *Angew. Chem., Int. Ed.* **2007**, *46*, 5144–5147.
- (32) Park, J. S.; Jeong, S.; Chang, D. W.; Kim, J. P.; Kim, K.; Park, E. K.; Song, K. W. *Chem. Commun.* **2011**, *47*, 4736–4738.
- (33) Jiang, L.; Yan, Y.; Huang, J. *Soft Matter* **2011**, *7*, 10417–10423.
- (34) Brinkhuis, R. P.; Rutjes, F. P. J. T.; van Hest, J. C. M. *Polym. Chem.* **2011**, *2*, 1449–1462.
- (35) Walde, P.; Cosentino, K.; Engel, H.; Stano, P. *ChemBioChem* **2010**, *11*, 848–865.
- (36) Zhou, Y. F.; Yan, D. Y. *Angew. Chem., Int. Ed.* **2004**, *43*, 4896–4899.
- (37) Ravoo, B. J.; Darcy, R. *Angew. Chem., Int. Ed.* **2000**, *39*, 4324–4326.
- (38) Dong, D. X.; Baigl, D.; Cui, Y. L.; Sinay, P.; Sollogoub, M.; Zhang, Y. M. *Tetrahedron* **2007**, *63*, 2973–2977.
- (39) Felici, M.; Marza-Perez, M.; Hatzakis, N. S.; Nolte, R. J. M.; Feiters, M. C. *Chem.—Eur. J.* **2008**, *14*, 9914–9920.
- (40) Falvey, P.; Lim, C. W.; Darcy, R.; Revermann, T.; Karst, U.; Giesbers, M.; Marcelis, A. T. M.; Lazar, A.; Coleman, A. W.; Reinhoudt, D. N.; Ravoo, B. J. *Chem.—Eur. J.* **2005**, *11*, 1171–1180.
- (41) Zhang, H.; Xin, F.; An, W.; Hao, A.; Wang, X.; Zhao, X.; Liu, Z.; Sun, L. *Colloid Surf. A-Physicochem. Eng. Asp.* **2010**, *363*, 78–85.
- (42) Tao, S.; Yueming, L.; Huacheng, Z.; Jianye, L.; Feifei, X.; Li, K.; Aiyou, H. *Colloids Surf., A* **2011**, *375*, 87–95.
- (43) Sun, L.; Zhang, H.; An, W.; Hao, A.; Hao, J. *J. Inclusion Phenom. Macrocyclic Chem.* **2010**, *68*, 277–285.
- (44) Liu, G. Y.; Jin, Q. A.; Liu, X. S.; Lv, L. P.; Chen, C. J.; Ji, J. A. *Soft Matter* **2011**, *7*, 662–669.
- (45) Jiang, L. X.; Peng, Y.; Yan, Y.; Huang, J. B. *Soft Matter* **2011**, *7*, 1726–1731.
- (46) Guo, X.; Li, H.; Gong, Z. Y.; Zhang, F. M.; Zheng, S. Y.; Gu, R. *J. Polym. Sci., Polym. Chem.* **2008**, *46*, 7491–7504.
- (47) Uda, R. M.; Tanabe, T.; Nakahara, Y.; Kimura, K. *Soft Matter* **2008**, *4*, 560–563.
- (48) Yin, H. Q.; Lei, S.; Zhu, S. B.; Huang, J. B.; Ye, J. P. *Chem.—Eur. J.* **2006**, *12*, 2825–2835.
- (49) Yin, H. Q.; Zhou, Z. K.; Huang, J. B.; Zheng, R.; Zhang, Y. Y. *Angew. Chem., Int. Ed.* **2003**, *42*, 2188–2191.
- (50) Chen, Q.; Schonherr, H.; Vancso, G. J. *Small* **2010**, *6*, 2762–2768.
- (51) Vanyur, R.; Biczok, L.; Miskolczy, Z. *Colloids Surf., A* **2007**, *299*, 256–261.
- (52) Fu, S. Z.; Chen, Q. D.; Shen, X. H. *Acta Phys.-Chim. Sin.* **2011**, *27*, 1913–1918.
- (53) Gonzalez-Gaitano, G.; Rodriguez, P.; Isasi, J. R.; Fuentes, M.; Tardajos, G.; Sanchez, M. *J. Inclusion Phenom. Macrocyclic Chem.* **2002**, *44*, 101–105.
- (54) Zhang, Y. M.; Deng, X. R.; Wang, L. C.; Wei, T. B. *J. Macromol. Sci., Part A: Pure Appl. Chem.* **2008**, *45*, 289–294.
- (55) He, Y. F.; Shen, X. H.; Chen, Q. D.; Gao, H. C. *Phys. Chem. Chem. Phys.* **2011**, *13*, 447–452.
- (56) Jiao, H.; Goh, S. H.; Valiyaveetil, S. *Macromolecules* **2002**, *35*, 3997–4002.
- (57) Sun, S.; Chen, X.; Liu, J.; Yan, J. L.; Fang, Y. *Polym. Eng. Sci.* **2009**, *49*, 99–103.
- (58) Debnath, S.; Shome, A.; Das, D.; Das, P. K. *J. Phys. Chem. B* **2010**, *114*, 4407–4415.
- (59) Zhao, Y. R.; Chen, X.; Jing, B.; Wang, X. D.; Ma, F. M. *J. Phys. Chem. B* **2009**, *113*, 983–988.
- (60) Park, C.; Lee, K.; Kim, C. *Angew. Chem., Int. Ed.* **2009**, *48*, 1275–1278.
- (61) Sun, T.; Li, Y. M.; Zhang, H. C.; Li, J. N.; Xin, F. F.; Kong, L.; Hao, A. Y. *Colloids Surf., A* **2011**, *375*, 87–96.
- (62) Batra, D.; Hay, D. N. T.; Firestone, M. A. *Chem. Mater.* **2007**, *19*, 4423–4431.
- (63) Yan, Y.; Jiang, L. X.; Huang, J. B. *Phys. Chem. Chem. Phys.* **2011**, *13*, 9074–9082.
- (64) Israelachvili, J. N.; Mitchell, D. J.; Ninham, B. W. *J. Chem. Soc., Faraday Trans. 2* **1976**, *72*, 1525–1568.